New Insight into the Formation of Structural Defects in Poly(Vinyl Chloride)

Jindra Purmova, Kim F. D. Pauwels, Wendy van Zoelen, Eltjo J. Vorenkamp, and Arend J. Schouten*

Department of Polymer Science, University of Groningen, Nijenborgh 4, 9747 AG Groningen, The Netherlands

Michelle L. Coote*

Research School of Chemistry, Australian National University, Canberra ACT 0200, Australia

Received January 7, 2005; Revised Manuscript Received May 9, 2005

ABSTRACT: The monomer conversion dependence of the formation of the various types of defect structures in radical suspension polymerization of vinyl chloride was examined via both ^{1}H and ^{13}C NMR spectrometry. The rate coefficients for model propagation and intra- and intermolecular hydrogen abstraction reactions were obtained via high-level ab initio molecular orbital calculations. An enormous increase in the formation of both branched and internal unsaturated structures was observed at conversions above 85%, and this is mirrored by a sudden decrease in stability of the resulting PVC polymer. Above this threshold-conversion, the monomer is depleted from the polymer-rich phase, and the propagation rate is thus substantially reduced, thereby allowing the chain-transfer processes to compete more effectively. In contrast to the other defects, the chloroallylic end groups were found to decrease at high conversions. On the basis of the theoretical and experimental data obtained in this study, this decrease was attributed to copolymerization and abstraction reactions that are expected to be favored at high monomer conversions. Finally, a surprising increase in the concentration of the methyl branches was reported. Although a definitive explanation for this behavior is yet to be obtained, the involvement of transfer reactions of an intra- or intermolecular nature seems likely, and (in the latter case) these could lead to the presence of tertiary chlorine in these defects.

Introduction

It is well-known that the thermal stability of poly(vinyl chloride) (PVC) is much lower than should be expected on the basis of its regular chemical structure.[1] Despite this, PVC products are employed in many applications, and this is facilitated by the use of heavy metal stabilizers, which provide the necessary protection against heat, light, and weathering.[2] Unfortunately, such compounds have a strong negative impact on the environment, especially after incineration, and thus the European PVC manufacturers have signed a voluntary commitment to reduce their use.[3] While there are more environmentally friendly stabilizers available, they are less effective and can affect (among other things) the early color of the material.[4] Improvements to the inherent stability of PVC would thus be desirable.

Because of the commercial importance of PVC, a number of studies[5,6] have previously been carried out on its thermal degradation. The main conclusion of these studies was that a decrease in stability is caused by irregularities in the structure of the polymer, in turn formed by secondary reactions during the radical polymerization process (see Schemes 1−4). The chlorine atoms contained in these irregular structures tend to eliminate easily, thereby converting them to initiation sites in the degradation process. Suppression of the side reactions by modifications to the polymerization process should thus lead to PVC with enhanced thermal stability.

* Authors to whom correspondence should be addressed. E-mail: a.j.schouten@rug.nl (A.J.S.); mcoote@rsc.anu.edu.au (M.L.C.).

Scheme 1. End Groups Formed by Termination by Disproportionation or Transfer to Monomer

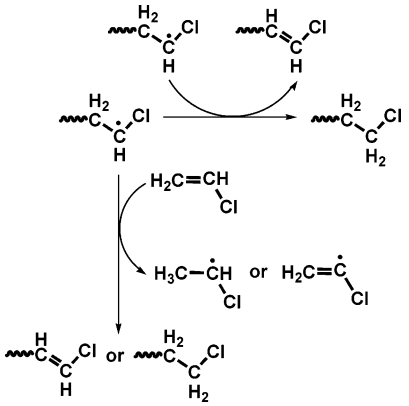

The most labile structural defects are internal allylic and tertiary chlorine functional groups formed by hydrogen-transfer reactions of an inter- or intramolecular nature,[6−12] (see Scheme 3, 4). There are other irregular structures present in PVC such as methyl and ethyl branches or chloroallylic end groups (Scheme 2). Although these latter structures are not thought to influence the thermal stability, they are nonetheless relevant to an understanding of the kinetics of the process.

Previous studies of vinyl chloride polymerization have indicated that the frequency of the side reactions is primarily influenced by the temperature,[6] the type of polymerization process used (eg., bulk, suspension, or solution polymerization),[13] the monomer conversion,[13] and pressure.[6,14] In the studies made on polymers

10.1021/ma050035p CCC: $30.25
Published on Web 06/18/2005

Scheme 2. Formation of Defect Structures after Head to Head Addition

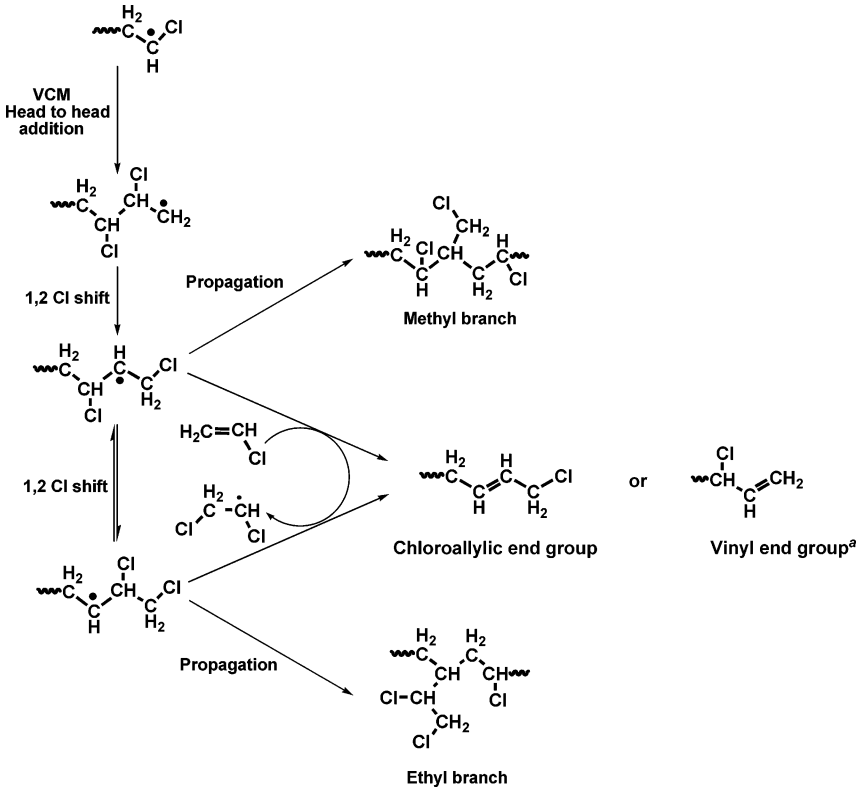

[a] Structure suggested by Llauro-Darricades et al.[36]

obtained at subsaturation conditions using emulsion PVC as a seed and a water soluble initiator,[6] it was found that the concentration of long-chain, butyl and ethyl branches increases with decreasing monomer pressure and increasing polymerization temperature, while the number of methyl branches decreases. In a similar study,[14] the decrease in the number of chloroallylic end groups and increase in the number of internal unsaturations with decreasing monomer pressure was reported. The type of polymerization process also has a major impact on the PVC microstructure. Radical suspension polymerization, which is the most common process in the PVC industry, is known to give rise to a lower concentration of unsaturations and branches (especially butyl branches) than solution polymerization.[13]

In this work, we study the effect of monomer conversion on the nature and concentrations of structural defects in radical suspension polymerization of vinyl chloride. Although the conversion dependence has been studied previously, this was done in a completely different polymerization system at subsaturation conditions when special precautions were taken to avoid diffusion control of the propagation.[6,14] PVC made by suspension polymerization was also analyzed in the past, but the conversion range was not covered completely and the low-molecular-weight part was extracted[13] or only some of the defects were taken in account.[15] There does not appear to be any detailed information on the formation of structural defects at high conversion under conditions that would normally be encountered in the industrial production of PVC via radical suspension polymerization.

The formation of structural defects as a function of monomer conversion was monitored using ^{1}H and ^{13}C NMR spectrometry. To assist in the interpretation of the results, the 1,2-intramolecular and corresponding intermolecular hydrogen abstraction reactions were also studied using high-level ab initio molecular orbital calculations.

Experimental Section

Materials. Vinyl chloride monomer (VCM, nominal purity 99.97%) was supplied by Shin Etsu PVC BV, The Netherlands. Partially hydrolyzed poly(vinyl acetate) (PVA, Alcotex B72, 72.5% hydrolysis) was provided by Harlow Chemical Company LTD, UK. Dimyristil peroxydicarbonate (Perkadox 26-W40, 40 wt % suspension in water) was received from Akzo Nobel Polymer Chemicals BV, The Netherlands. Buffer ($NaH_2PO_4 \cdot 2H_2O$ p.a.), tetrahydrofuran (THF, 99+%, inhibited with 250 ppm BHT), and azo-bis-isobutyronitrile (AIBN) were obtained from Acros Organics. A terminating agent prepared as 10 wt % solution of 2,2-bis-4-hydroxyphenylpropane in methanol, crotyl chloride (nominal purity 96%), Bu_3SnH, Bu_3SnD, and THF-d_8 were obtained from Aldrich. Nitrogen gas of a purity of 99.999% was used, while water was purified in our lab by reverse osmosis (RO-water). $LiAlH_4$, *p*-xylene, 1,2,4-trichlorobenzene, and benzene-d_6 were purchased from Merck. All chemicals for polymerization, reductive dehalogenation, and analysis were used as received, without further treatment.

Polymerization. Vinyl chloride monomer was polymerized by suspension polymerization in a 1 L steel autoclave (type HPM-P-1 from Premex Reactor AG, Switzerland). The reaction vessel was filled with 350 mL of water partially hydrolyzed poly(vinyl acetate), buffer salt, and in some experiments, crotyl chloride. Air was then removed by flushing with nitrogen and subsequent application of reduced pressure. VCM (175 g) was added and the temperature was increased to 57.5 °C (polymerization temperature), while the dimyristil peroxydicarbonate initiator was added. During the polymerization of VCM, the anchor stirrer was set at 1000 rpm. Once the desired monomer conversion (monitored by decrease of VCM pressure) was reached, the termination agent was added, and the reactor was cooled to 21 °C. After removing residual VCM, the product mixture was filtered, and the PVC powder was washed with

Scheme 3. Reactions Occurring during the Propagation of Radical VC Polymerization, Intramolecular Hydrogen Transfer

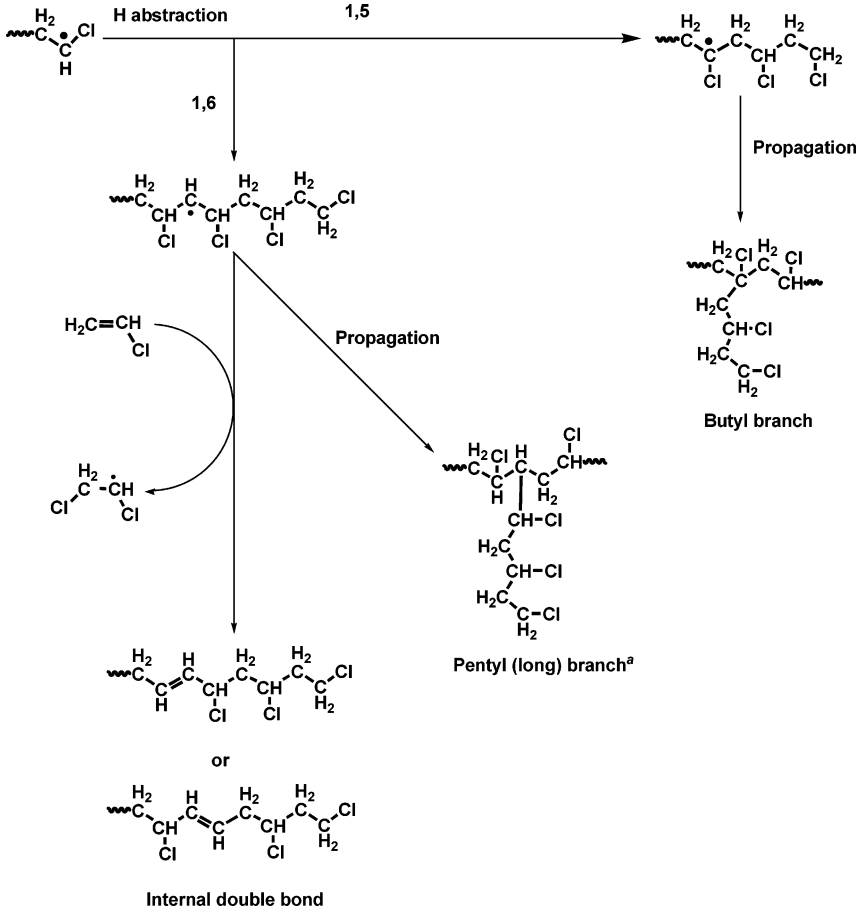

[a] Further propagation of the radical formed by 1,6 backbiting would give rise to a pentyl branch. According to Hjertberg et al., only branches up to 5 carbons can be distinguished using ^{13}C spectra of reductively dehalogenated PVC.[8] This structure would give the same peaks as long branches formed by intermolecular transfer.

RO-water and dried overnight at 55 °C in a vacuum. Monomer conversion was then determined by gravimetry.

Reductive Dehalogenation. The presence of Cl, and its consequent tacticity, renders undetectable the ^{13}C signals of carbons contained in the different types of branches. To address this problem, the PVC polymer was reduced to its corresponding hydrocarbon because the ^{13}C spectra of such polymers can provide the desired information.[8,16] Reductive dehalogenation (on the basis of a free radical mechanism) was used for this purpose because it is relatively quick and does not affect the original microstructure of the polymer.[16,17] The one-step modification[17] of the original method developed by Starnes et al.[16] was applied using Bu_3SnH or Bu_3SnD as reduction agent, AIBN as the initiator, and *p*-xylene and THF as solvents. THF was distilled under argon with addition of $LiAlH_4$ to inhibit the formation of peroxides. The resulting product was precipitated with an excess of cold methanol and filtered. The precipitate was redissolved in *p*-xylene, and a few drops of concentrated HCl were added until the solution became clear. The mixture was then added to cold methanol, containing a few mL of HCl. The second precipitation step was performed to eliminate tin compounds formed during the reaction. The degree of reduction of the PVC was determined by integration of the signals of methylenic and methynic carbons in ^{13}C NMR spectra.

Gel Permeation Chromatography. Molecular weight distributions were determined by gel permeation chromatography (GPC) carried out using a Spectra Physics chromatograph equipped with 2 PL-Gel Mixed C columns, a Viscotek H-502 online viscometer, and a Shodex RI-71 refractive index detector and Trisec software. All measurements were performed at 25 °C in THF. A universal calibration curve was constructed using narrow MWD polystyrene standards, fitted with a fifth-order polynomial. A conventional calibration method, using the Mark Houwink constants $a = 0.7155$, $\log K = -3.9003$ for polystyrene, and $a = 0.769$, $\log K = -3.8079$ for PVC, was employed.[18]

Dehydrochlorination Test. The thermal stability of the resins was determined with the aid of the dehydrochlorination test (DIN 53 381; ISO 182-3:1993), performed in the analytical laboratory of Shin Etsu PVC BV, Pernis, The Netherlands. The sample was degraded at 180 °C under an N_2 flow rate of 120 mL min^{-1}. The HCl formed during this process was purged through distilled water, the conductivity of which was measured continuously as a function of time. The resulting curves provide information about the time of initiation of the degradation (t_i) and the time necessary for a change in conductivity of 50 $\mu S\ cm^{-1}$ (t_{st}). This latter quantity corresponds to a weight loss of 0.05%, and the dehydrochlorination rate (dhc rate) was determined by dividing 0.05% by the time needed to achieve this weight loss ($t_{st} - t_i$).

NMR. ^1H and ^{13}C spectra were obtained on a 500 MHz VARIAN-INOVA spectrometer. Pre-acquisition delays were optimized and digital signal processing was used to obtain a flat baseline for accurate integration. The samples for the ^1H NMR experiments were prepared as approximately 5% w/v solution of PVC in THF-d_8. The standard ^1H pulse sequence was run at 45 °C using a tip angle of 80°. Assignment of the signals in the ^1H spectra (known from literature[19]) was confirmed by ^1H homonuclear COSY experiments.[20]

Proton-decoupled ^{13}C spectra of reductively dehalogenated samples were run at 120 °C for approximately 10% w/ solutions in the mixture of 1,2,4-trichlorobenzene and benzene-d_6 (3:1). The tip angle was 60°, pulse repetition time was 5 s, and

Scheme 4. Reactions Occurring during the Propagation of Radical VC Polymerization, Intermolecular Hydrogen Transfer

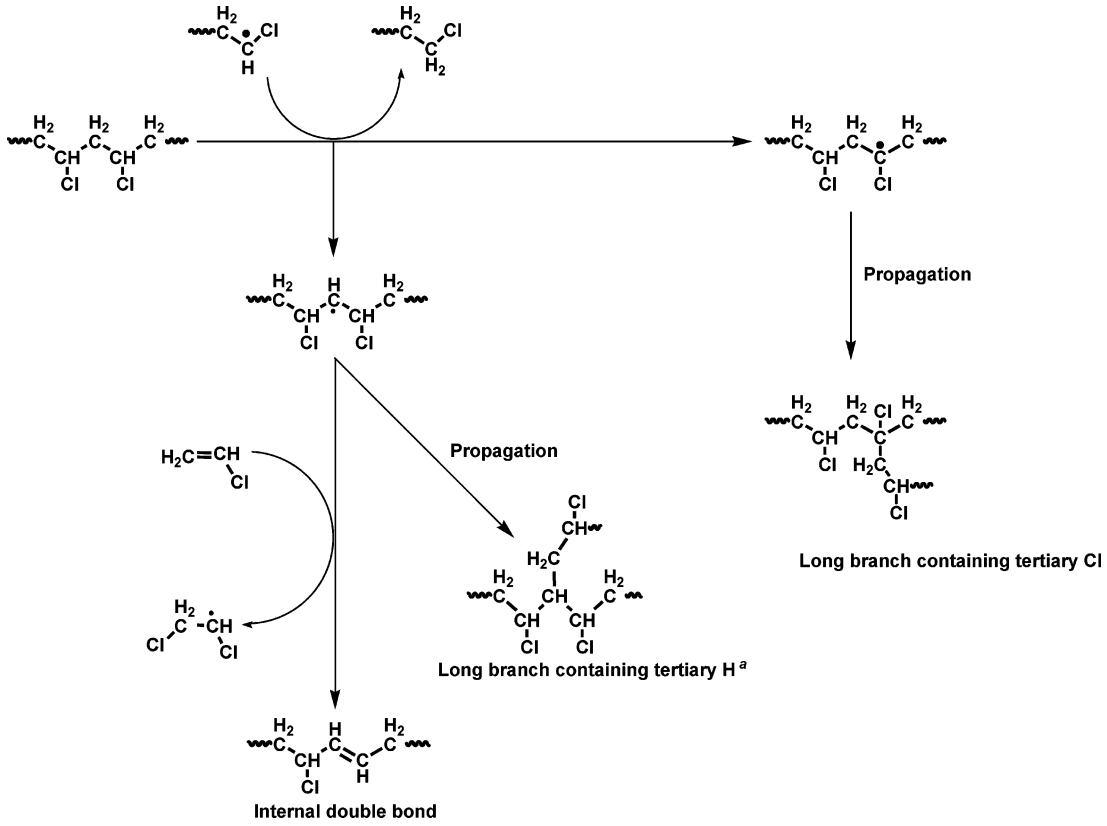

[a] Branch structure proposed by Hjertberg et al.[8]

broadband decoupling was used. The relaxation time T_1 of the main chain $-CH_2-$ resonance was measured as 1.6 s, somewhat higher than reported by Starnes et al.[10] The peaks were identified using the spectra of model compounds[8,21] and by means of computer simulations.[22]

The concentrations of the defects were usually expressed as the numbers per 1000 VC units, and their calculation was based on integration of the corresponding peaks in both ^{1}H and ^{13}C spectra.[8,19] Determination of the concentration of the branches was based on the intensities of the carbons at position α to the branch-point carbon. In the case of end groups, the results were expressed as numbers per chain to include the influence of differences in average degree of polymerization at lower and higher conversions. Number per chain = (number per 1000 VC * average degree of polymerization)/1000.

Although at least 99% of all chlorine atoms were removed from the PVC samples, the presence of partially reduced methyl and butyl branches in some of the samples could not be neglected, and this was taken in account when calculating the number of defects. The highest values of the standard deviations calculated from at least three independent ^{1}H NMR measurements were taken as the estimated experimental error (0.01−0.05). The standard deviation of the concentration of different types of branches was calculated by comparing the ^{13}C spectra, collected by using different pulse intervals or decoupling methods (result 0.08−0.13).

Ab Initio Molecular Orbital Calculations. Standard ab initio molecular orbital theory[23] and density functional theory[24] calculations were carried out using GAUSSIAN 03[25] and MOLPRO 2000.6.[26] Calculations were performed at a high level of theory, which was chosen on the basis of recent assessment studies for addition and abstraction reactions.[27,28] Geometries of the reactants, products, and transition structures were optimized at the MPW1K/6-31+G(d,p) level of theory, and zero-point vibrational energy (scaled by a factor of 0.9515)[29] was also calculated at this level. To ensure that the geometries were global, rather than merely local minimum energy structures, alternative conformations were first screened at this level. Improved energies were calculated at the G3-(MP2)-RAD level of theory.[30] This is a high-level composite procedure that approximates coupled cluster energies [URCCSD(T)] with a large triple-ζ basis set by using additivity approximations. This method has been demonstrated to reproduce the experimental heats of formation of a variety of open- and closed-shell species within approximately 1 kcal mol^{-1}.[30]

Having obtained the G3(MP2)-RAD barriers at 0 K, the gas-phase rate coefficients for the addition and transfer reactions were calculated at 57.5 °C via standard transition state theory, in conjunction with the rigid rotor/harmonic oscillator approximation. The entropies of activation ($\Delta S^{\ddagger}$) were calculated using the MPW1K/6-31+G(d,p) optimized geometries, and scaled MPW1K/6-31+G(d,p) frequencies were used to calculate the zero-point vibrational energy, the temperature correction to the barrier, and the vibrational contribution to $\Delta S^{\ddagger}$. Standard textbook formulas,[31] on the basis of the statistical thermodynamics of an ideal gas, were used for this purpose.[32]

Corrections for quantum mechanical tunneling were calculated using the Eckart tunneling method.[33] In this method, the minimum energy path for the reaction is approximated using an Eckart function, for which the one-dimensional Schrödinger equation has an analytical solution. In the present work, we fitted the Eckart function to the curvature of the minimum energy path of the reaction at the transition structure, as measured using the imaginary frequency.[34] A detailed assessment of the accuracy of one-dimensional tunneling methods for these reactions has not as yet been published; however, there are some preliminary indications that, for moderate levels of tunneling, this method provides reasonably accurate tunneling corrections, comparable to those obtained using more sophisticated multidimensional treatments.[35]

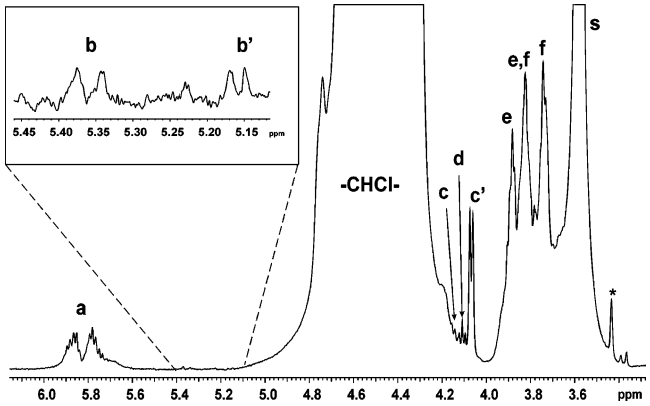

Figure 1. Typical ^{1}H NMR spectrum of PVC sample synthesized at 57.5 °C in the Laboratory of Polymer Chemistry, University of Groningen. (a) $-CH{=}CHCH_2Cl$, $-CH{=}CHCHCl-$, $-CHClCH{=}CH_2$, and $-CHClCH{=}CHCl$; (b) $-CHClCH{=}CHCl$; (b′) $-CH_2CCl{=}CH_2$ or (b and b′) $-CHClCH{=}CH_2$; (c and c′) *cis*- and *trans*- $-CH{=}CHCH_2Cl$; (d) $-CH_2CH_2O(CO)-$(initiator end group); (e) $-CHClCH_2Cl$; (f) $-CH_2CH_2$-Cl and $-CH_2Cl$ methyl branch; s, solvent; * ^{13}C satellite.

Results and Discussion

^{1}H Peak Assignments. A typical ^{1}H NMR spectrum for the PVC produced in the present work is provided in Figure 1. As can be seen in this figure, several "defects" are present in the polymer, including saturated end groups, branches, and various unsaturated structures. Previous studies[9,13,14] of the radical suspension polymerization of vinyl chloride have suggested that the unsaturated structures present in the resulting PVC polymer are chloroallylic end groups $-CH{=}CH-CH_2$-Cl and internal double bonds $-CHCl-CH{=}CH-CH_2-$. Such groups would arise through various types of chain transfer to polymer or monomer reactions (see Schemes 2−4). Signals corresponding to these types of protons have been identified in the present polymers between $\delta = 5.6$ and 6.0 ppm (see Figure 1).

In addition, we also detected very weak signals downfield to the −CHCl− peak and upfield to the signals of double bonds, which have not as yet been identified. These peaks were visible in the spectra of all PVC samples, but their intensity was much higher in the spectra of low-molecular-weight fractions, indicating that they are likely to be end groups. The peak located at 5.36 ppm was unambiguously assigned with the aid of a cross-peak (with coordinates 5.35 and 6.00 ppm) found in the COSY 45 spectrum (see Figure 2). According to the computer simulations,[22] the chemical shift of the saturated CHCl proton neighboring with a double bond is around 5.3 ppm, while the unsaturated protons in a double bond where a chlorine atom is also present have a chemical shift around 6 ppm. The peak thus belongs to the methynic proton in the saturated CHCl part of $-CHClCH{=}CHCl$ end group. This structure can be formed by transfer of a head-to-tail macroradical to monomer or by disproportionation (Scheme 1). The other peak, located at 5.16, was assigned to protons located in the end groups $-CH_2CCl{=}CH_2$ formed by reinitiation of the radical formed by transfer of the head-to-tail macroradical to the monomer (see Scheme 1). Presence of the so-called vinyl end group $-CHClCH{=}CH_2$ (which is proposed to form via abstraction of Cl from a radical formed after head-to-head addition,[36] see Scheme 2) was excluded because of the absence of the correlation between CH and CH_2 unsaturated hydrogens in the COSY spectrum (Figure 2).

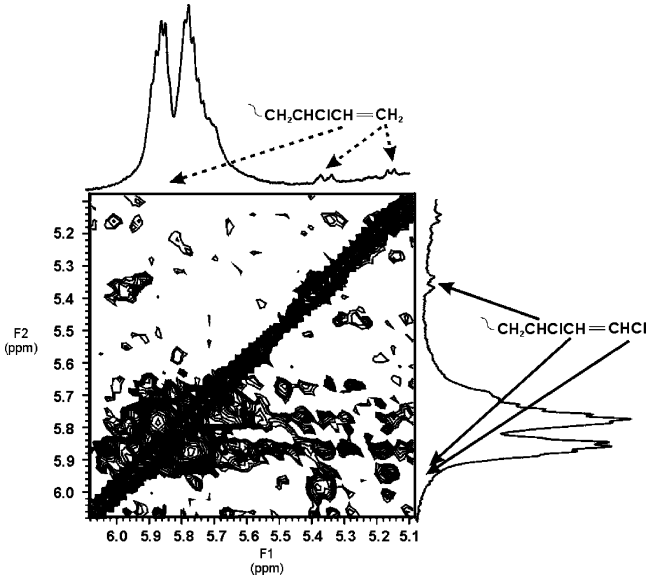

Figure 2. Expansion of the region of unsaturated protons of COSY 45 spectrum of low-molecular-weight fraction of 23.7% conversion PVC sample synthesized in the Laboratory of Polymer Chemistry, University of Groningen.

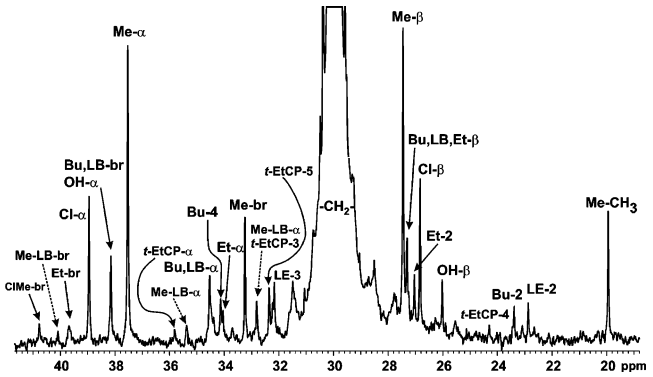

Figure 3. ^{13}C NMR spectrum of PVC synthesized at 57.5 °C in the Laboratory of Polymer Chemistry, University of Groningen, reductively dehalogenated with Bu_3SnH. Me = methyl, ClMe = chloromethyl, Et = ethyl, Bu = butyl, LB = long branch; LE = long chain end, Me-LB = vicinal methyl and long branch. Br = branch-point carbon; α, β = positions of the carbons in the main chain with respect to the branch-point carbon, 1−4 = positions of the carbons in the corresponding branch with respect to the branch-point carbon, where lower the number, the more remote the carbon.

The protons located within the unsaturated part of the $-CHClCH{=}CHCl$ are also expected to overlap with the multiplet corresponding to the total area of unsaturated protons. Nonetheless, taking into account the intensity of the −CHCl− part of the above-mentioned end group (Figure 1), their contribution would be almost negligible.

^{13}C Peak Assignments. The presence of methyl, ethyl, butyl, and longer alkyl branches was detected in ^{13}C spectra of samples reduced with Bu_3SnH (Figure 3). Signals of cyclopentane moieties formed by cyclization of double bonds during the reduction process[37] (chloroallylic end groups; t-EtCP, *trans*-1-ethyl-2-(long alkyl) cyclopentane) were also present, as well as the peaks that ensued from the carbons in $-CH_2CH_2CH(OH)CH_2CH_2-$ segments. This structure, reported previously by Wescott et al.,[38] arises from the sequential reduction of the $-CH_2CHCl(CO)CH_2CHCl-$ structures with $LiAlH_4$ and Bu_3SnH. Carbonyl groups are intro-

Scheme 5. Alternative Reactions Leading to Formation of Methyl and/Or Ethyl Branches

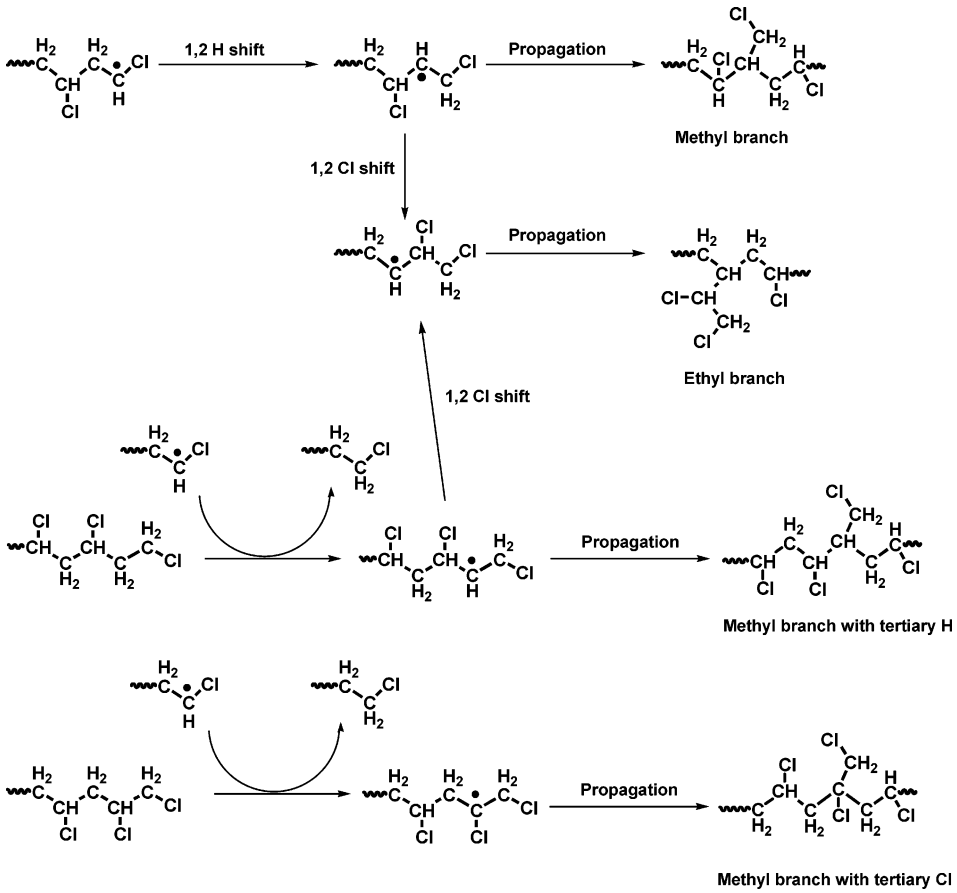

duced into the PVC chain by copolymerization with carbon monoxide, which is formed in situ from the reactions of residual oxygen with radicals.[39] The amount of CO can be determined indirectly by measuring the concentration of HCl, the other product of such reactions.[40] The evacuation method applied prior to the polymerization gave a chloride concentration of 12.3 ppm, which would give 0.01 CO groups per 1000 VC units, a concentration far below the detection limit of ^{13}C NMR. Nonetheless, the peaks belonging to the hydroxyl-containing segments were clearly present in our spectra. Hydroxyl groups come in our case probably from poly(vinyl alcohol) used as a suspending agent.

According to the literature,[8,10] butyl and some of the long-chain branches carry a tertiary Cl on their branch-point carbon. This fact was also confirmed by analysis of ^{13}C spectra of PVC reduced with Bu_3SnD, where the signals of the carbons to which the Cl was originally attached usually appear as triplets (spectrum available in Supporting Information). The same spectrum also showed methyl and ethyl branches that had an H on the branch-point carbon (see the Supporting Information), which is an indication that head-to-head addition and subsequent Cl shifts and propagation are the origin of these branches (see Scheme 2). However, it should be noted that this is also consistent with methyl branches formed via a possible 1,2-intra- or intermolecular hydrogen abstraction reaction (see Scheme 5). Methyl branches containing a tertiary Cl may also be formed via an intermolecular hydrogen abstraction from the β-carbon of the dead polymer (see Scheme 5). Unfortunately, these could not be identified by analysis of ^{13}C spectra of the Bu_3SnD-reduced polymer because the *t*-EtCP-3 signal has the same chemical shift (32.81 ppm) as the triplet, arising from the branch-point carbon of such methyl branches (33.23(Me-br) − 0.4(isotope shift) = 32.83 ppm). The chemical shifts and corresponding isotope shifts of the carbons found in the reduced samples are given in Supporting Information.

Conversion Dependence of the Defect Structures. On the basis of the ^{1}H and ^{13}C NMR spectra, the concentrations of the various defect structures were followed as a function of monomer conversion. The conversion dependence of the unsaturated end groups (−CHClCH=CHCl) is plotted in Figure 4, from which it is seen that the number of these end groups per polymer molecule (chain) reached its minimum around 70% conversion, where the contribution of the excess Trommsdorff effect (which, as manifested by decrease

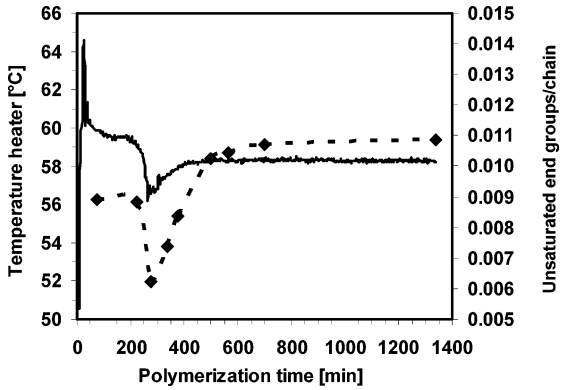

Figure 4. Development of the number of unsaturated end groups −CHClCH=CHCl per chain (-- -◆-- -) and temperature of the heater (solid line) during suspension polymerization of VCM at 57.5 °C.

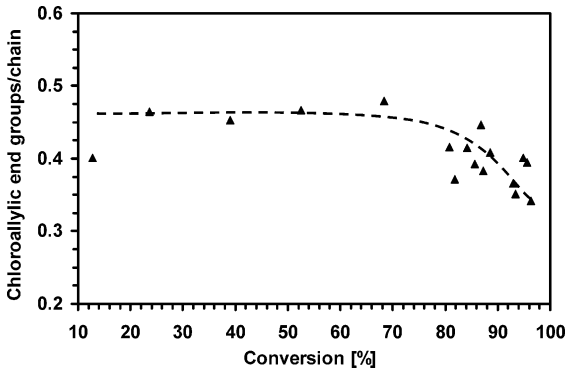

Figure 5. Dependence of the number of chloroallylic end groups per chain on monomer conversion in suspension PVC made at 57.5 °C.

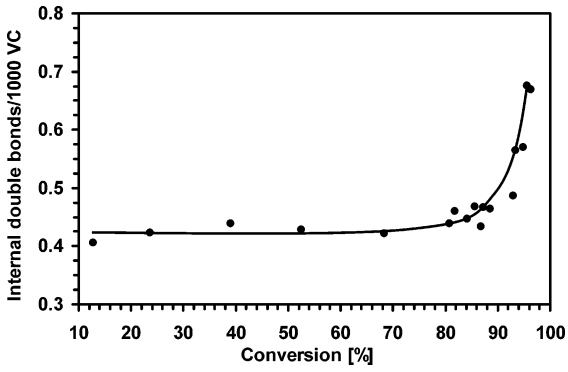

Figure 6. Dependence of the number of internal double bonds per 1000 VC units on conversion in suspension PVC made at 57.5 °C.

Scheme 6. Copolymerization of Chloroallylic End Groups

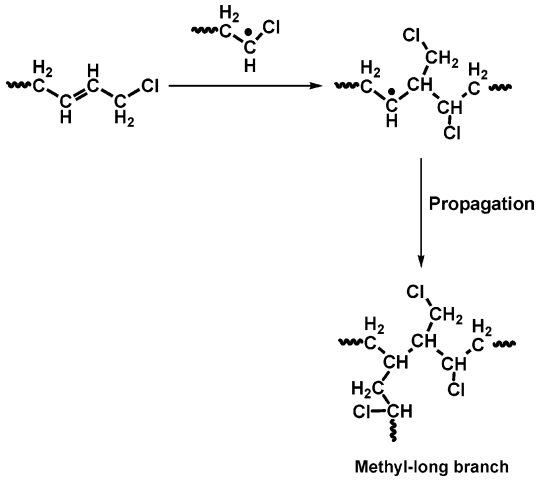

in the heater temperature, begins at ~40% and finishes at ~85% conversion) attains its maximum.[41] Because the bimolecular terminations are known to be suppressed during the Trommsdorff effect, this confirms the assignment of the minor peak at 5.36 ppm to the methynic proton contained in −C*H*ClCH=CHCl end group (see section Peak Assignments).

The conversion dependence of the chloroallylic end groups per chain is plotted in Figure 5. These were initially relatively constant as a function of monomer conversion, presenting practically no change until approximately 70% of monomer conversion, then the number of these defects *decreased*. The copolymerization of chloroallylic end groups with the growing polymer chain (see Scheme 6), and their conversion to internal unsaturated groups via hydrogen abstraction reactions (see Scheme 7), could explain this downtrend. This will be discussed in more detail further in the text.

The number of internal unsaturations remained relatively constant as a function of monomer conversion until around 85%; at which point, a steep increase occurred (see Figure 6). This trend is also mirrored by the branched structures (Figure 7). The number of long-chain branches showed the largest relative increase: 108%, followed by butyl (26%), ethyl (20%), and methyl branches (19%). It should be noted that, in the case of the ethyl branches, establishing the exact magnitude of the increase is complicated by the low concentration of this type of branching. The experimental error in the ^{13}C NMR is estimated to be 0.13 branch/1000 VC; that means approximately 26% in the case of the number of ethyl branches. Nonetheless, it is clear from Figure 7 that the concentrations of all of the branched structures increase above 85% conversion.

Scheme 7. Reactions of the Allylic Radical Formed by Hydrogen Abstraction from the Carbon Atom Adjacent to the Double Bond in Crotyl Chloride

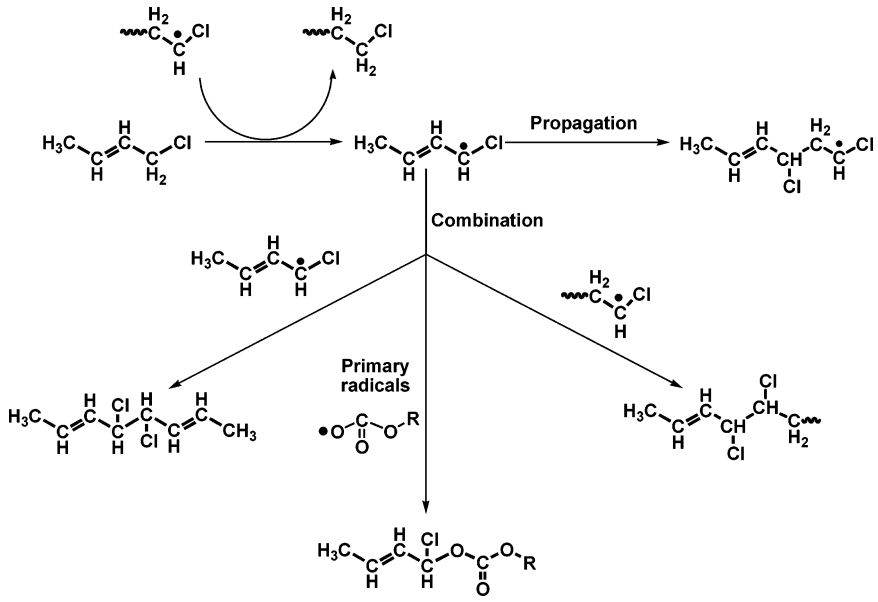

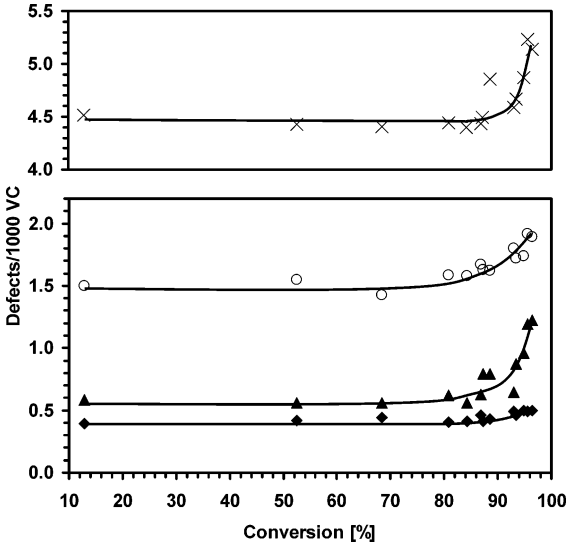

Figure 7. Dependence of the number of different types of branches per 1000 VC units on conversion in suspension PVC made at 57.5 °C. Methyl branches (×); butyl branches (○); long branches (▲); ethyl branches, (◆).

Internal double bonds are known to originate in either inter- or intramolecular abstraction of H from the $-CH_2-$ group of the polymer chain, followed by reaction with VCM by chlorine atom β-scission,[9,12,14] while long chain and butyl branches are known to originate in inter- or intramolecular hydrogen-transfer reactions, followed by propagation (see Schemes 3 and 4). The sharp increase in these defect structures at 85% conversion thus implies a large increase in the rates of these chain-transfer reactions. As will be discussed below, this increase can be understood in terms of the reduction of monomer concentration and the concurrent increase in polymer concentration in the polymer-rich phase at conversions above 85%.

However, the sharp increase in methyl and ethyl branches is more surprising. The ethyl branches are thought to form via propagation of the radical, resulting from two subsequent Cl shifts after head-to-head monomer addition (see Scheme 2).[42] The methyl branches may form if the same radical propagates after just one Cl shift.[43] Although the probability of head-to-head addition might be expected to remain relatively constant throughout the polymerization process, the probability that the radical undergoes subsequent Cl shifts might have been expected to increase as the propagation rate declines under conditions of monomer starvation. Although this provides a possible explanation for the increases in methyl and ethyl branches, other observations suggest that, for the production of methyl branches, an additional mechanism may also be at work. In particular, we noted that addition of 3 wt % *o*-dichlorobenzene to the VC monomer during polymerization caused a decrease in the number of butyl branches,[44] defects known to be formed by intramolecular H abstraction.[8,10] In contrast, *o*-dichlorobenzene had little effect on the concentration of long branches and ethyl branches,[44] where the defects are not formed by intramolecular hydrogen abstraction. Surprisingly, addition of *o*-dichlorobenzene caused a decrease of the concentration of methyl branches at conversions >85%,[44] thereby indicating that an intramolecular hydrogen shift (which would have to be a 1−2 shift in this case) might play a role.

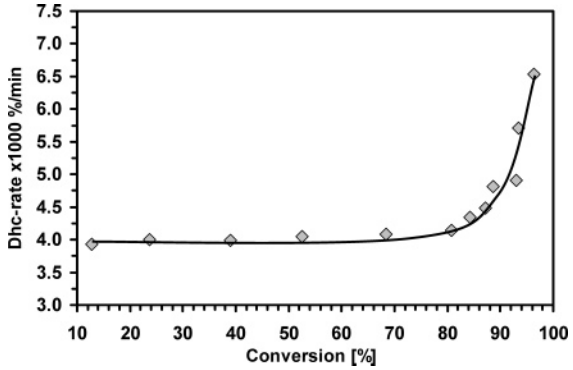

Figure 8. Development of the dehydrochlorination rate with monomer conversion in suspension PVC made at 57.5 °C.

The 1−2 hydrogen-transfer reaction has been rejected in several publications,[45,46] arguing that such a type of hydrogen migration has never been observed for alkyl radicals in solution.[47] The mechanism was also discounted on the basis of the ^{13}C spectrum of a reductively dehalogenated PVC sample obtained by polymerization of α−deuterated monomer.[46] In the latter case, it was shown that signals corresponding to the deuterium-labeling pattern expected for the methyl branch formed by further propagation of a radical, resulting from a 1−2 hydrogen shift were absent. However, it is worthwhile to note that the polymerization of deuterated monomer[46] was carried out in solution, and the increase of the number of methyl branches begins at ∼85% monomer conversion, far beyond the critical conversion (Figure 7). As we discuss below, under such conditions, the concentration of polymer chains is extremely high,[48] and the monomer has to diffuse to the polymer-rich phase from the vapor phase and the suspension medium. As a result, the propagation rate decreases dramatically, and intramolecular transfer reactions (of all types) might be expected to compete more effectively with propagation. A 1−2 hydrogen shift may thus be feasible under these circumstances, and in this work we use ab initio calculations to investigate this possibility.

It is important to note that this sudden increase in the structural defects at high conversions plays an important role in the thermal stability of the polymer. In fact, the increase in the dehydrochlorination rate for the PVC polymer as a function of conversion (Figure 8) mirrors the increase in the concentration of the internal unsaturated structures (Figure 6) and butyl and long branches (Figure 7). This confirms the close connection between allylic and tertiary chlorines and thermal stability reported earlier.[6,14]

Ab Initio Molecular Orbital Calculations. Some of the more intriguing results of the present work are the observations that, at a high conversion, (a) there is a large increase in methyl branches that might arise in a 1−2 hydrogen shift, and (b) there is a decline in the concentration of the chloroallylic end groups, indicating that they may undergo copolymerization. To examine the feasibility of these unusual reactions, an ab initio molecular orbital study was also undertaken.

Barriers, enthalpies, entropies, and rate coefficients (at 57.5 °C) were calculated for both the intramolecular 1−2 hydrogen shift (1) and the corresponding intermolecular transfer reaction (2) with the dead polymer, and also the propagation of the chloroallylic end group (3). So that the calculations could be performed at a high level of theory, the propagating species and correspond-

Scheme 8. Model Reactions Used in the Calculation of the Rate Coefficients for: (1) The 1−2 Intramolecular Hydrogen Abstraction Reaction, (2) The Intermolecular 1−2 Intramolecular Hydrogen Abstraction Reaction, (3) The Copolymerization of the Chloroallylic End Groups, and (4) The Propagation Rate

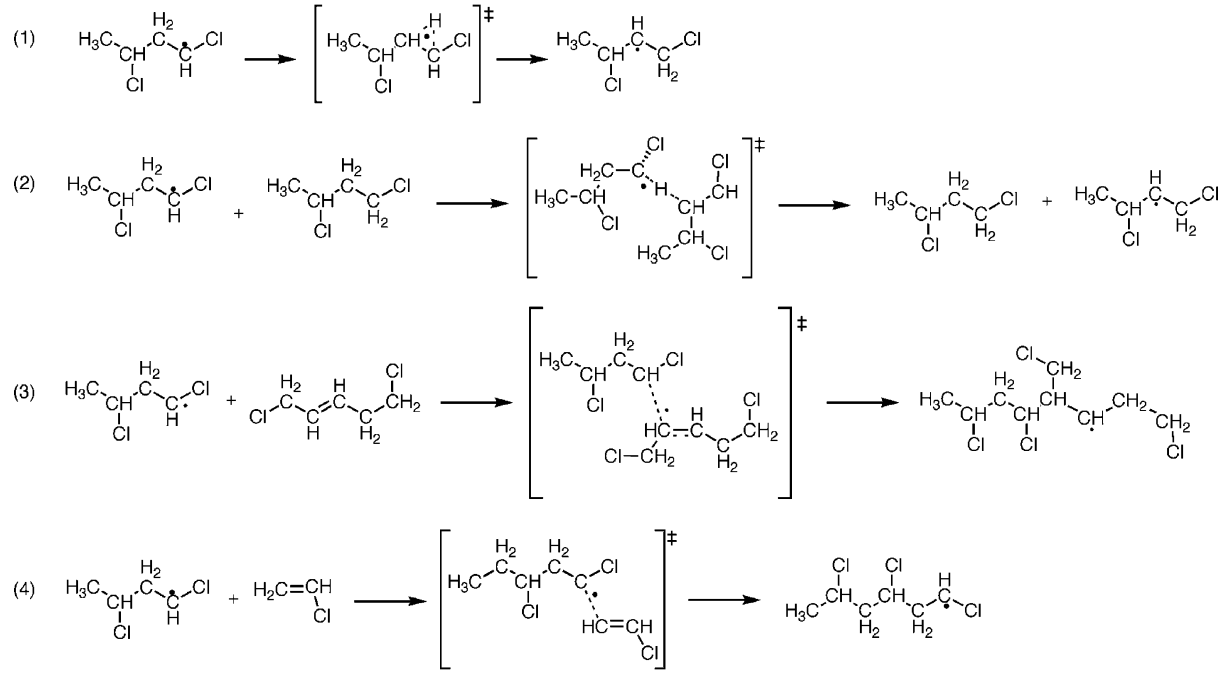

Table 1. Calculated Kinetic and Thermodynamic Parameters for the Propagation, Copolymerization, Intramolecular, and Intermolecular 1−2 Hydrogen-Transfer Reactions of the Vinyl Chloride Propagating Radical at 0 and 330.65 K[a]

	intramolecular (1)			intermolecular (2)			propagation (3)	coplymerization of chloroallylic end group (4)
	fwd[b]	rev[c]	overall[d]	fwd[b]	rev[c]	overall[d]	fwd[b]	fwd[b]
ΔH_0 (kJ mol^{-1})	180.5	176.9	3.5	41.0	37.4	3.5	12.6	12.5
$\Delta H_{330.65}$ (kJ mol^{-1})	180.0	175.8	4.2	41.8	37.6	4.2	11.6	12.0
$\Delta S_{330.65}$ (J mol^{-1} K^{-1})	−4.5	−13.3	8.9	−161.4	−170.3	8.9	−159.4	−171.0
$\Delta G_{330.65}$ (kJ mol^{-1})	181.5	180.2	1.2	95.1	93.9	1.2	64.3	68.6
$Q_{330.65}$	4.9×10^3	4.9×10^3		2.8×10^1	2.8×10^1		1	1
$k_{330.65}$	7.2×10^{-13}	1.1×10^{-12}	0.64	4.8	7.6	0.64	1.3×10^4	2.8×10^3

[a] Calculated at the G3(MP2)-RAD//MPW1K/6-31+G(d,p) level of theory. Rate coefficients (k) were calculated using simple transition-state theory and incorporate Eckart tunneling corrections (Q) (see text). The intramolecular reaction 1 proceeds via transition structure **1** in Figure 9, and its forward and reverse rate coefficients have the units s^{-1}. The intermolecular reaction 2 proceeds via transition structure **2** in Figure 9, and its forward and reverse rate coefficients have the units L mol^{-1} s^{-1}. The propagation reaction 3 proceeds via transition structure **3** in Figure 9, and its forward and reverse rate coefficients have the units L mol^{-1} s^{-1}. [b] Forward direction. [c] Reverse direction. [d] Overall enthalpy/entropy change for the reaction. The k value in this context refers to the (dimensionless) equilibrium constant for the reaction.

ing dead polymer were modeled as dimers (see Scheme 8). To "benchmark" the calculations, and enable chain-transfer coefficients and reactivity ratios to be calculated, the corresponding propagation reaction 4 of the vinyl chloride dimer was also studied. The key kinetic and thermodynamic parameters for reactions 1−4 (see Scheme 8) are provided in Table 1, while the geometries of all species are shown schematically in Figure 9. Full geometries, in the form of GAUSSIAN archive entries are provided in the Supporting Information.

Examining Table 1, we first note that the calculated propagation rate coefficient (1.3×10^4 L mol^{-1} s^{-1}) is in excellent agreement with the reported experimental value (1.2×10^4 L mol^{-1} s^{-1}).[49] This agreement is unlikely to be fortuitous because calculations at a similar level of theory have recently reproduced the experimental propagation rate for a different system, methyl acrylate.[50] Moreover, the accuracy of the electronic structure calculations themselves has been separately verified against a large test set of gas-phase experimental data[30] and in extensive assessment studies for radical addition and abstraction reactions.[27,28] For these reasons, it seems reasonable to suppose that the calculated rate coefficients in Table 1 are both reliable and relevant to the polymeric system.

From Table 1, it is seen that the intramolecular 1−2 shift is, not unsurprisingly, a relatively unfavorable reaction. If we compare it with corresponding intermolecular reaction, we note that, on an enthalpic basis, the intermolecular shift is overwhelmingly preferred, the respective enthalpies of activation being 180.0 kJ mol^{-1} and 41.8 kJ mol^{-1}. This reflects the high degree of strain in the three-membered transition structure for the intramolecular shift, in which the C−H−C angle is 69°, a long way from its preferred linear arrangement. However, on an entropic basis, the intramolecular shift is preferred over the intermolecular reaction. This is mainly because the intramolecular shift is a unimolecular reaction, and therefore does not "lose" 3 translational and 3 external rotational modes upon reaction, as in the bimolecular intermolecular transfer reaction. This additional entropy loss in the intermolecular reaction is

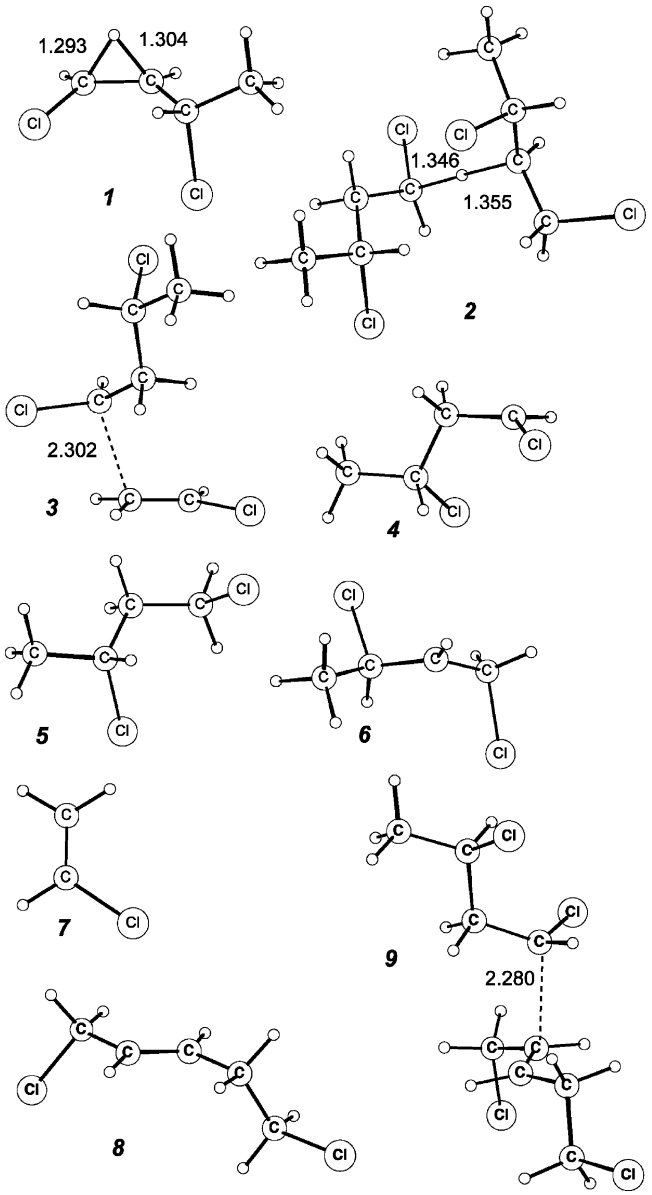

Figure 9. MPW1K/6-31+G(d,p) optimized geometries of the transition structures for the intramolecular 1−2 hydrogen transfer (1), the corresponding intermolecular hydrogen transfer (2), and the propagation (3) reactions of the model vinyl chloride propagating radical (4). Also shown are the geometries of the corresponding vinyl chloride "polymer" (5), the radical product (6) of the 1−2 hydrogen shifts, vinyl chloride monomer (7), chloroallylic end group (8), and the addition of the propagating PVC radical to the double bond of the chloroallylic end group (9).

only partially compensated for by the additional vibrational entropy of the larger and more flexible intermolecular transition structure, and hence the intramolecular shift is preferred on an entropic basis. Nonetheless, the enthalpic effects dominate, and the intermolecular shift is strongly preferred (by approximately 13 orders of magnitude at 330.65 K).

When we compare the rate coefficients for the chain-transfer reactions with the propagation rate coefficient, it is clear that under normal conditions, the formation of *methyl branches* via intramolecular 1−2 hydrogen abstraction would be a relatively rare occurrence in vinyl chloride polymerization. For example, in a bulk monomer (i.e., with a monomer concentration of around 11.6 mol L^{-1}), the intramolecular 1−2 shift would occur once every 2×10^{17} propagation steps. Of course, at high conversions, the monomer concentration (particularly in the polymer-rich phase) would be much lower than this, and the relative frequency of the intramolecular reaction would increase. This would be further enhanced if propagation were to become diffusion limited. However, as we will demonstrate below, even when these factors are considered, it is unlikely that a 1−2 hydrogen shift is primarily responsible for the formation of the methyl branches.

The intermolecular hydrogen shift may be a more feasible route to methyl branches. At low conversion, hydrogen abstraction from the dead polymer would occur only rarely because the monomer concentration would greatly exceed the polymer concentration. However, as a monomer is depleted, this reaction would compete more effectively. Thus, for example, if the (molar) polymer and monomer concentrations were equal, the formation of methyl branches via a intermolecular hydrogen abstraction from the β-carbon would occur once every 2700 propagation steps; under conditions of monomer starvation, yet higher frequencies of abstraction would be possible. However, it is important to note that the intermolecular abstraction of hydrogens from other positions on the (dead) polymer chain (i.e., leading to ethyl, propyl, butyl, and longer branches) should also occur with a similar frequency, and thus one should have expected the total concentration of the long branches to be orders of magnitude greater than that of the methyl branches, which is not the case. Although intermolecular abstraction reactions will contribute to the production of methyl branches (and all other types of branches), they are unlikely to be the predominant mechanism.

Finally, it appears that the copolymerization of the chlorallylic end groups may be feasible under the right conditions. The chloroallylic end group is approximately 1 order of magnitude less reactive than the double bond of the monomer (see Table 1), a feature that arises mainly in entropic factors. Using the propagation rates for the chloroallylic group (k_{pc}) and the normal propagation step (k_p), the calculated reactivity ratio of the chloroallylic group ($r_c = k_p/k_{pc}$) is 4.7. Although one might expect on this basis that the propagation of the chloroallylic end group could compete with normal propagation, it must be remembered that, at low conversions, the concentration of the monomer is orders of magnitude higher than that of the chloroallylic end group, and the reaction is not significant. However, at high conversions, if the monomer concentration in the polymer droplets diminishes, the propagation of the chloroallylic end group could become more significant.

Chain-Transfer Kinetics at a High Conversion. The present results indicate that there is a large increase in the concentration of branches and internal unsaturations in the polymer at conversions above 85%. This in turn suggests that there is a large increase in the frequency of inter- and intramolecular chain-transfer reactions above this "threshold-conversion". In what follows, we argue that this is explicable in terms of the reduction of the monomer concentration and the concurrent increase in polymer concentration in the polymer-rich phase at conversions above 85%.

It is characteristic for suspension and bulk processes that, after a critical conversion, the polymerization is taking place exclusively in the polymer-rich phase.[51] According to Ravey et al.[52] the polymer-rich phase is

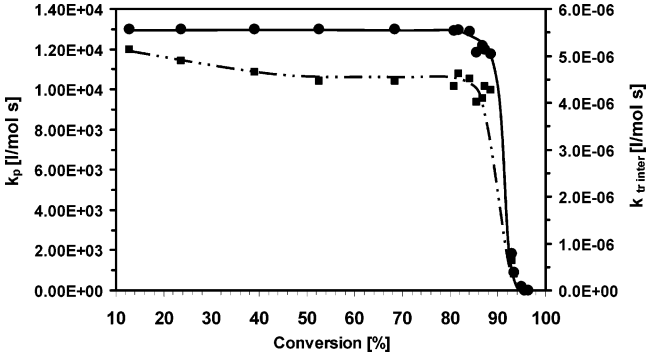

Figure 10. Calculated apparent rate coefficients in a polymer-rich phase at 57.5 °C vs monomer conversion (propagation (●) k_p, intermolecular transfer (■) $k_{tr\ inter}$).

much less swollen in the monomer at conversions higher than 85%. As a result of this decrease in monomer concentration, the rate of propagation is substantially reduced while, concurrently, the concentration of polymer (available for intermolecular chain transfer to polymer reactions) increases, thereby allowing chain transfer to compete more effectively with the propagation step.

Another feature of the polymerizations where phase separation takes place (which is the case in the suspension polymerization of vinyl chloride) is the reduced mobility of the polymer chains. This also contributes to a decrease in the rates of the propagation and *inter*-molecular transfer, which become diffusion rather than chemically controlled. Rate coefficients are then composed from the terms k_{chem} (rate coefficient corresponding to chemically controlled reaction) and k_{diff} (diffusion contribution), having the following relationship:[53]

$$\frac{1}{k_{obs}} = \frac{1}{k_{chem}} + \frac{1}{4\pi\sigma_m D_i N_A} \qquad (1)$$

The first term of this expression can be evaluated using the ab initio k_{chem} values for propagation and intermolecular transfer reactions from Table 1. The second term of the equation based on the Smoluchowski model[54] accounts for the diffusion contribution, where σ_m[55] $= 4.69 \times 10^{-10}$ m stands for Lennard−Jones diameter of a monomer molecule, N_A for Avogadro constant, and D_i for self-diffusion coefficient of monomer (D_m) or polymer (D_p). The self-diffusion coefficients are governed by the preexponential factor and activation energy necessary to make a diffusional jump, together with a free volume contribution. The preexponential factor of the monomer was calculated with the aid of the Dullien equation.[56] The preexponential factors in the diffusion of the polymer molecules were determined via reptation theory,[57] and the segmental motion of the radical chain end due to the propagation was also considered.[55] Free volume contributions were calculated using free volume theory.[58] The complete methodology was extensively described elsewhere.[59] The resulting calculated apparent values for the rates of propagation and intermolecular chain transfer (to polymer) in the polymer-rich phase, as a function of conversion, are provided in Figure 10.

Both the propagation (k_p) and intermolecular transfer ($k_{tr\ inter}$) rate coefficients showed a dramatic decrease beyond 85% conversion (Figure 10). However, the high concentration of polymer molecules and low concentration of the monomer (see Figure 11) compensate for the

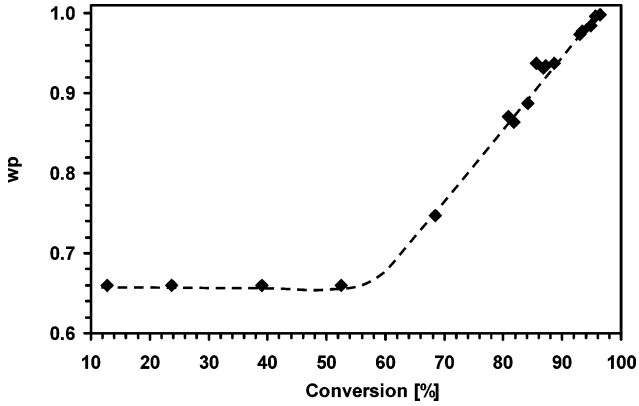

Figure 11. Development of the weight fraction of PVC in polymer-rich phase during suspension polymerization of VCM at 57.5 °C. Weight fraction of polymer (w_p) was calculated using the model developed by Xie et al.[48]

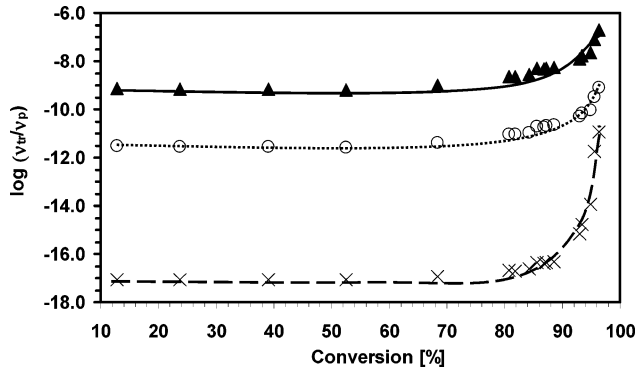

Figure 12. Correlation of the ratios of propagation rate and different transfer reactions rates in polymer-rich phase with monomer conversion during suspension VCM polymerization at 57.5 °C: intermolecular (▲); 1−2 intramolecular hydrogen transfer (×); copolymerization of chloroallylic end groups (○).

low value of $k_{tr\ inter}$. This is reflected in the development of the ratio of the intermolecular hydrogen-transfer rate to the propagation rate ($\nu_{tr\ inter}/\nu_p$) with the monomer conversion (Figure 12), which is clearly in favor of intermolecular transfer at conversions above 85%. The increasing $\nu_{tr\ inter}/\nu_p$ ratio above the critical conversion can thus account for the dramatic increase in long-chain branches and internal unsaturations. However, it is important to note that the formation of internal unsaturations also involves a transfer to the monomer step (Schemes 3 and 4), and the frequency of this step would be expected to decrease at high conversions, in an analogous manner to the propagation step. Because the formation of internal unsaturations increases, rather than decreases, at high conversions, the intermolecular hydrogen abstraction reaction must be the rate-determining step for the formation of internal double bonds.

The $\nu_{tr\ intra}/\nu_p$ ratio also increases substantially at high conversions because of the declining propagation rate. In this regard, it should be noted that, because the intramolecular reactions are unlikely to become diffusion controlled, their rates should remain relatively constant as a function of conversion, and the increase in $\nu_{tr\ intra}/\nu_p$ at a high conversion should be even more pronounced than the increase in the $\nu_{tr\ inter}/\nu_p$ ratio. Figure 12 also shows the development of the $\nu_{tr\ intra}/\nu_p$ ratio with conversion for the 1−2 shift; similar profiles would be expected for the possible intramolecular transfer reactions, though the absolute values of these

ratios would, of course, be different for the various shifts. This increasing $\nu_{tr\ intra}/\nu_p$ ratio accounts satisfactorily for the increases in butyl branches at high conversions and might, in principle, also provide an explanation for the increasing methyl branches. However, when we examine the magnitude of the $\nu_{tr\ intra}/\nu_p$ ratio for the 1−2 shift, it becomes obvious that, despite the low propagation rate at high conversions, the propagation rate is still substantially greater than the rate of the intramolecular chain-transfer reaction. The value of $\nu_{tr\ intra}/\nu_p$ for this reaction was 1.14×10^{-11} at the highest achievable conversion (96.4%), when the weight fraction of monomer in the polymer-rich phase is only 0.001. The intramolecular shift would thus participate only marginally to the formation of methyl branches at high monomer conversions.

It should be noted, in contrast to the present work, it has been argued elsewhere[12,60] that propagation is *not* diffusion controlled up to conversions of at least 90% at the temperature of the present study. This conclusion was based largely on the observation that, in contrast to the current results, the butyl branch concentrations in previous studies[6,12,42,60] depend only the temperature and monomer concentration during the polymerization. However, the reaction conditions in these studies differ from those of the present work (and hence the industrial process), and these differences are likely to delay the onset of diffusion control. In particular, Hjertberg et al.[6] used a high agitation speed to avoid the diffusion control of the propagation, and Starnes et al.[12,42,60] considered the formation of branched defects in solution polymerization, and at subsaturation conditions before the agglomeration of primary particles occurred. The contrasting results of the present work indicate that, in the industrial process, the onset of diffusion control (and associated decline in stability of the polymer) may occur at earlier conversions than previously supposed.

Copolymerization of Chloroallylic End Groups. Prior to the current work, it was generally accepted that reactions following head-to-head emplacement are responsible for the formation of methyl and ethyl branches and chloroallylic end groups[42,61,62] (see Scheme 2). In the absence of other reactions leading to these defects, the number of methyl branches should decrease, the number of ethyl branches increase, and the number of chloroallylic end groups should stay constant with decreasing monomer concentration.[6,42] However, it is clear from Figure 5 that this is not the case. The concentration of chloroallylic end groups actually decreased after 85% of the monomer conversion (Figure 5), and the number of methyl and ethyl branches increased (Figure 7).

The chloroallylic chain ends are not normally thought to be very reactive, but on the basis of our ab initio calculations (Table 1), the rate coefficient for radical addition to the chloroallylic double bond is only 4.6 times lower than the propagation rate coefficient. Of course, at a low conversion, the concentration of the monomer in the polymer droplets is orders of magnitude greater than that of the chloroallylic end groups, and the rate copolymerization reaction is not significant. However, under conditions of monomer starvation, copolymerization may become feasible. Such a reaction would give rise to a methyl branch with a neighboring long branch (Scheme 6). In previous studies by other research groups, structures of this nature have not been identified in the spectra of reduced PVC (on the basis of their predicted peak assignments).[8,63] However, in the present work, we suggest different locations for these structures in the ^{13}C NMR and, on the basis of these peak assignments, we can provide experimental evidence for this reaction.

According to our predictions,[22] the chemical shift of the branch-point carbon should be 40.8 ppm for the methyl branch and 41.4 ppm for the long branch. Carbons in the α position to the methyl and long branches should be situated at 35.2 and 32.7 ppm, respectively. The ^{13}C chemical shifts of branch-point carbons should thus differ enough from carbon chemical shifts of the branches and cyclic structures formed from the unsaturations[12,37] normally present in NMR spectra of reductively dehalogenated samples (see also Table S1 in Supporting Information and discussion further in the text). A small but clear peak is observed at 32.7 ppm, and less defined signals appear at 35.2 and 40.2 ppm in the spectra of dehalogenated specimens of all monomer conversions (Figure 3). A conceivable source of one of the Me-LB-br resonance could be the quaternary alkyl carbon of the bisphenol A that was used to terminate the polymerization. However, we can rule this out because the signal of this carbon lies at 42.5 ppm in the reference spectrum of this compound. Moreover, the signals of aromatic carbons of bisphenol A at 116 and 128 ppm were not visible in the spectrum of reduced PVC.

Further experimental support for the copolymerization reaction was provided by examination of the reaction of a low-molecular-weight model compound for chloroallylic end groups with PVC macroradicals. Crotyl chloride ($CH_3-CH=CH-CH_2Cl$) was chosen for this purpose. Both 5 g and 1 g of crotyl chloride corresponding to around 19 (respectively 4) chloroallylic end groups/1000 VC considerably reduced the reaction rate, thus indicating that a disubstituted double bond is not inert toward both primary and macroradicals. Addition of the growing polymer chain to the double bond in crotyl chloride would give a vicinal methyl branch with theoretical chemical shifts of 42.7 ppm for the branch-point carbon and 37.1 ppm for the α carbon.[22] There are indeed very weak peaks having comparable chemical shifts in ^{13}C spectra of PVC polymerized with addition of crotyl chloride (Figure 13).

Although the model experiments provided evidence for copolymerization of the chloroallylic end groups, they also suggested additional reaction pathways for this group. In particular, besides propagation, hydrogen abstraction from a carbon atom adjacent to the double bond could also occur (Scheme 7). The radical formed in the abstraction reaction is not very reactive because of the resonance stabilization and is often capable only of combination reactions[64] (Scheme 7). The products of the combination reactions with crotyl chloride radicals or PVC macroradicals are predicted to have ^1H NMR signals overlapping with the signals of internal unsaturations and −CHCl− protons of the main chain. Polymers made with addition of crotyl chloride should thus present a higher content of internal double bonds than standard polymers of similar conversion. This is indeed the case; a subtle, but observable increase occurs (Figure S2 in Supporting Information). The theoretical chemical shift of the protons contained in −O−CHCl− moiety adjoining the double bond present in the combination product of primary and crotyl chloride radicals

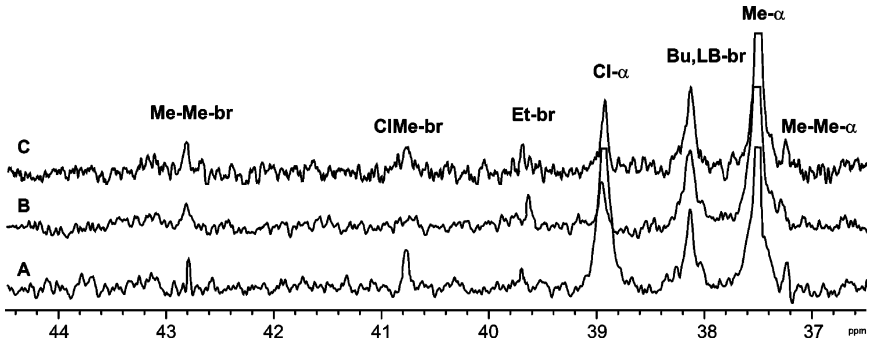

Figure 13. ^{13}C NMR spectra of reductively dehalogenated PVC polymerized with addition of (A) 5 g crotyl chloride; (B) 1 g crotyl chloride, and (C) 1 g crotyl chloride, three times longer polymerization time. Me-Me = vicinal methyl branches; br = branch-point carbon; α = position of the carbons in the main chain with respect to the branch-point carbon. See caption of the Figure 7 for the nomenclature of the other peaks.

is 7 ppm. An additional peak at 7.8 ppm absent in NMR spectra of standard PVC appears in the spectra of "crotyl-chloride-PVC" (Figure S3 in Supporting Information). Its intensity increases with the amount of crotyl chloride added to the reaction and with the polymerization time (Figure S4 in Supporting Information). Formation of low-reactive radicals by hydrogen abstraction from a chloroallylic functional group of crotyl chloride explains satisfactorily the retarding effect of this compound on VCM polymerization. Chloroallylic end groups are susceptible to the same hydrogen abstractions and subsequent combination reactions as crotyl chloride.[5,14,63] The absence of the peak corresponding to the product of combination with primary radicals can be explained by the low concentration of the chloroallylic end groups.

In summary, a combination of ab initio calculations and experimental studies indicate that the chloroallylic end groups are susceptible to propagation and transfer reactions; the former giving rise to methyl and long chain branches, the latter giving rise to additional internal unsaturations. At a high conversion, the reduction in the monomer concentration, and the associated decline in the propagation rate, allow these reactions to compete more effectively. This explains the observed decline in the concentration of chloroallylic end groups and contributes to the increasing concentration of branched structures and internal unsaturations.

Origin of the Methyl Branches. Thus far, we have provided an explanation for the increasing internal unsaturations and long-chain and butyl branches at a high conversion and the decreasing chloroallylic end groups. However, the origin of the methyl branches in high-conversion PVC remains unexplained. Although copolymerization of the chloroallylic end groups leads to methyl branches, the methyl branches formed by this reaction do not contribute to the observed increase in the concentration of methyl branches because of the different location of the respective peaks. Although, at a high conversion, the declining propagation rate allows all intramolecular hydrogen-transfer reactions to compete more effectively with propagation, the 1−2 hydrogen shift was found to be too unreactive to be a significant source of the observed methyl branches. Although intermolecular hydrogen transfer was found to provide a much more favorable route, it should be remembered that this process should also generate branches of any other specific length with a similar frequency, and hence the relative concentration of the long-chain branches should have been much higher than that of the methyl branches. In other words, the increase in methyl branches at a high conversion may thus be only *partially* explained via the increase intermolecular hydrogen-transfer reactions.

The increase in methyl (and ethyl) branches may simply reflect that, under conditions of monomer starvation, the radicals produced after head-to-head addition have a greater probability to undergo subsequent Cl shifts before propagation. However, as noted, the addition of 3 wt % *o*-dichlorobenzene to a VC monomer during polymerization has little effect on the ethyl branches, but causes a large decrease in the concentration of the methyl branches, suggesting that these are formed via different mechanisms. Interestingly, the addition of *o*-dichlorobenzene also causes a decrease in the butyl branches, suggesting that their mechanism of formation (which in the case of the butyl branches is an intramolecular hydrogen shift) is similar to that of the methyl branches. Although the 1−2 shift hydrogen was ruled out on the basis of (gas-phase) ab initio calculations, it is possible that, in the polymer-rich phase, the reaction is catalyzed via interactions involving substituents on (for example) the dead polymer chain, interactions that are disrupted by the addition of *o*-dichlorobenzene. Further investigations of this unusual solvent effect are currently underway.

Conclusions

In this work, we examined the conversion dependence of the formation of the various types of defect structures in radical suspension polymerization of vinyl chloride. It was found that, above 85% monomer conversion, there is an enormous increase in the formation of both branched and internal unsaturated structures, and this is mirrored by a sudden decrease in the stability of the resulting PVC polymer. The increased formation of these defects, which arise through various types of chain-transfer reaction, can be understood in terms of the locus of polymerization. The liquid monomer-rich phase is consumed, and the monomer has to diffuse to the polymer-rich phase from the vapor phase and suspension medium already above 60% conversion. However, the impact of these changes on the concentration of defect structures is observable at more than 20% higher monomer conversion. From our experimental and theoretical evidences, it can be deduced that, above this so-called threshold-conversion, the polymer-rich phase becomes extremely dense, making the diffusion coefficient of the monomer much lower than in the monomer-rich phase. This causes substantial reductions in the propagation rate, thereby allowing the chain-transfer processes to compete more effectively.

In contrast to the branched structures and internal unsaturations, the concentration of chloroallylic end groups was found to decrease at a high conversion. Chloroallylic end groups arise when the radical formed via head-to-head addition undergoes one or two subsequent Cl shifts, followed by transfer to the monomer (instead of propagation, which can lead to methyl or ethyl branches, respectively). Their rate of formation is not expected to decline at high conversions, and the decrease in their concentration is instead the result of their consumption in copolymerization and transfer reactions, the former giving rise to branched structures, the latter giving rise to internal unsaturations. The feasibility of these processes was confirmed via a combination of high-level ab initio calculations and experimental studies involving the model compound, crotyl chloride.

In addition, the present results provide evidence in favor of an alternative mechanism for the formation of methyl branches in PVC. Prior to the current work, it was generally accepted that reactions following head-to-head emplacement are responsible for the formation of methyl and ethyl branches, and that the ethyl branches should increase and the methyl branches should decrease at a high conversion.[6] However, we observed a significant increase in both the methyl and ethyl branches. These kinetic results, and additional evidence concerning the effect of *o*-dichlorobenzene, suggest that an additional mechanism for the formation of methyl branches, possibly on the basis of inter- and/or intramolecular hydrogen transfer. On the basis of ab initio molecular orbital calculations, the intermolecular route was favored, though it is likely that is only a partial explanation. The possibility that the 1−2 shift is being catalyzed via interactions involving (for example) the dead polymer cannot be ruled out, and further investigations of the effects of solvents on these systems are now underway. The 1−2 intermolecular hydrogen shift would result in a fraction of the methyl branches carrying a tertiary chlorine, and they may therefore be more significant for the thermal stability of PVC (especially at high monomer conversions) than was described earlier.

Acknowledgment. We would like to thank to Dutch Ministry of Economical Affairs (SENTER-IOP) for financial support and the members of the IOP steering committee and Dr. Katja Loos (University of Groningen) for helpful discussions. We also gratefully acknowledge generous allocations of computing time on the Compaq Alphaserver of the National Facility of the Australian Partnership for Advanced Computing and the Australian National University Supercomputing Facility and provision of an Australian Research Council postdoctoral fellowship (to M.L.C.).

Supporting Information Available: Table S1 shows the ^{13}C chemical shifts of an 87.2% conversion sample reduced with Bu_3SnH and Bu_3SnD, and the corresponding spectrum is provided in Figure S1; the content of internal double bonds in polymers made with addition of crotyl chloride is shown in Figure S2; Figure S3 contains the partial ^1H NMR spectrum of PVC made with addition of crotyl chloride, and Figure S4 provides the information about the correlation of the number of combination products of primary and crotyl chloride radicals with the amount of crotyl chloride added to the reaction and with the polymerization time; the MPW1K/6-31+G(d,p) optimized geometries, of the reactants, products, and transition structures, in the form of GAUSSIAN archive entries, are provided in Table S2, and associated total energies, zero-point vibrational energies, thermal corrections, and entropies are provided in Table S3. This material is available free of charge via the Internet at http://pubs.acs.org.

References and Notes

(1) Asahina, M.; Onozuka, M. *J. Polym. Sci., Polym. Chem. Ed.* **1964**, *2*, 3505−3513.
(2) See for example: Braun, D. *J. Vinyl Addit. Technol.* **2001**, *7*, 168−176.
(3) Vinyl 2010 Sustainable Development: Progress Report 2003. http://www.stabilisers.org/pr2003/PROGRESS%20REPORT%202003.pdf; 2003, p 13−14.
(4) Reviewed in: Steenwijk, J. (Natural) Polyols as Stabilisers for Heavy Metal-Free PVC: The Stabilising Mechanism and the Influence on Rheology, Dissertation, Utrecht University, 2003; pp 15−27.
(5) Starnes, W. H., Jr. *Prog. Polym. Sci.* **2002**, *27*, 2133−2170.
(6) Hjertberg, T.; Sörvik, E. M. ACS Symposium Series 280; American Chemical Society: Washington, DC, 1985; 259−284.
(7) Hjertberg, T.; Sörvik, E. M. *J. Macromol. Sci., Chem.* **1982**, *A17*, 983−1004.
(8) Hjertberg, T.; Sörvik, E. M. *Polymer* **1983**, *24*, 673−684.
(9) Hjertberg, T.; Sörvik, E. M. *Polymer* **1983**, *24*, 685−692.
(10) Starnes, W. H., Jr.; Schilling, F. C.; Plitz, I. M.; Cais, R. E.; Freed, D. J.; Hartless, R. I.; Bovey, F. A. *Macromolecules* **1983**, *16*, 790−807.
(11) Starnes, W. H., Jr.; Chung, H.; Wojciechowski, B. J.; Skillicorn, D. E.; Benedikt, G. M. *Polym. Prepr. (Am. Chem. Soc., Div. Polym. Chem.)* **1993**, *34*, 114−115.
(12) Starnes, W. H., Jr.; Zaikov, V. G.; Chung, H. T.; Wojciechowski, B. J.; Tran, H. V.; Saylor, K.; Benedikt, G. M. *Macromolecules* **1998**, *31*, 1508−1517.
(13) LLauro-Darricades, M.-F.; Bensemra, N.; Guyot, A.; Pétiaud, R. *Makromolekul. Chem., Macromol. Symp.* **1989**, *29*, 171−184.
(14) Starnes, W. H., Jr.; Chung, H.; Wojciechowski, B. J.; Skillicorn, D. E.; Benedikt, G. M. In *Polymer Durability: Degradation, Stabilization, and Lifetime Prediction*; Advances in Chemistry Series 249; American Chemical Society: Washington, DC, 1996, *249*, 3−18.
(15) Xie, T. Y.; Hamielec, A. E.; Rogestedt, M.; Hjertberg, T. *Polymer* **1994**, *35*, 1526−1535.
(16) Starnes, W. H., Jr.; Hartless, R. I.; Schilling, F. C.; Bovey, F. A. *Polym. Prepr. (Am. Chem. Soc., Div. Polym. Chem.)* **1977**, *18*, 499−504.
(17) Hjertberg, T.; Wendel, A. *Polymer* **1982**, *23*, 1641−1645.
(18) Skillicorn, D. E.; Perkins, G. G. A.; Slark, A.; Dawkins, J. V. *J. Vinyl Technol.* **1993**, *15*, 105−108.
(19) LLauro-Darricades, M.-F.; Guyot, A. *J. Macromol. Sci., Chem.* **1986**, *A23*, 221−269.
(20) Marion, D.; Wuthrich, K. *Biochem. Biophys. Res. Commun.* **1983**, *113*, 967−974.
(21) Starnes, W. H., Jr. *Macromolecules* **1985**, *18*, 1780−1786.
(22) (a) *ACD/CNMR Predictor,* version 3.50; Advanced Chemistry Development Inc.: Toronto, 1998. (b) *Chem Draw Ultra,* version 8.0.3; CambridgeSoft Corporation: Cambridge, MA, USA, 2003.
(23) Hehre, W. J.; Radom, L.; Schleyer, P. v. R.; Pople, J. A. *Ab Initio Molecular Orbital Theory*; Wiley: New York, 1986.
(24) Koch, W.; Holthausen, M. C. *A Chemist's Guide to Density Functional Theory*; Wiley-VCH: Weinheim, 2000.
(25) Frisch, M. J.; Trucks, G. W.; Schlegel, H. B.; Scuseria, G. E.; Robb, M. A.; Cheeseman, J. R.; Montgomery, Jr., J. A.; Vreven, T.; Kudin, K. N.; Burant, J. C.; Millam, J. M.; Iyengar, S. S.; Tomasi, J.; Barone, V.; Mennucci, B.; Cossi, M.; Scalmani, G.; Rega, N.; Petersson, G. A.; Nakatsuji, H.; Hada, M.; Ehara, M.; Toyota, K.; Fukuda, R.; Hasegawa, J.; Ishida, M.; Nakajima, T.; Honda, Y.; Kitao, O.; Nakai, H.; Klene, M.; Li, X.; Knox, J. E.; Hratchian, H. P.; Cross, J. B.; Bakken, V.; Adamo, C.; Jaramillo, J.; Gomperts, R.; Stratmann, R. E.; Yazyev, O.; Austin, A. J.; Cammi, R.; Pomelli, C.; Ochterski, J. W.; Ayala, P. Y.; Morokuma, K.; Voth, G. A.; Salvador, P.; Dannenberg, J. J.; Zakrzewski, V. G.; Dapprich, S.; Daniels, A. D.; Strain, M. C.; Farkas, O.; Malick, D. K.; Rabuck, A. D.; Raghavachari, K.; Foresman, J. B.; Ortiz, J. V.; Cui, Q.; Baboul, A. G.; Clifford, S.; Cioslowski, J.; Stefanov, B. B.; Liu, G.; Liashenko, A.; Piskorz, P.; Komaromi, I.; Martin, R. L.; Fox, D. J.; Keith, T.; Al-Laham, M. A.; Peng, C. Y.; Nanayakkara, A.; Challacombe, M.; Gill, P. M. W.; Johnson, B.; Chen, W.; Wong, M. W.; Gonzalez, C.;

Pople, J. A. *Gaussian 03*, Revision C.02; Gaussian, Inc., Wallingford CT, 2004.
(26) Werner, H.-J.; Knowles, P. J.; Amos, R. D.; Bernhardsson, A.; Berning, A.; Celani, P.; Cooper, D. L.; Deegan, M. J. O.; Dobbyn, A. J.; Eckert, F.; Hampel, C.; Hetzer, G.; Korona, T.; Lindh, R.; Lloyd, A. W.; McNicholas, S. J.; Manby, F. R.; Meyer, W.; Mura, M. E.; Nicklass, A.; Palmieri, P.; Pitzer, R.; Rauhut, G.; Schütz, M.; Stoll, H.; Stone, A. J.; Tarroni, R.; Thorsteinsson, T. *MOLPRO* version 2000.6; University of Birmingham: Birmingham, 1999.
(27) Coote, M. L., *J. Phys. Chem. A* **2004**, *108*, 3865−3872.
(28) Gómez-Balderas, R.; Coote, M. L.; Henry, D. J.; Radom, L. *J. Phys. Chem. A* **2004**, *108*, 2874−883.
(29) Lynch, B. J.; Truhlar, D. G. *J. Phys. Chem. A* **2001**, *105*, 2936−2941.
(30) Henry, D. J.; Sullivan, M. B.; Radom, L. *J. Chem. Phys.* **2003**, *118*, 4849−4860.
(31) See for example: (a) Stull, D. R.; Westrum, E. F. Jr.; Sinke, G. C. *The Thermodynamics of Organic Compounds*; John Wiley & Sons: New York, 1969. (b) Robinson, P. J. *J Chem. Educ.* **1978**, *55*, 509−510. (c) Steinfeld, J. I.; Francisco, J. S.; Hase, W. L. *Chemical Kinetics and Dynamics*; Prentice Hall: Englewood Cliffs, New Jersey, 1989.
(32) These are summarized in the Supporting Information of the recent publication: Coote, M. L.; Radom, L. *Macromolecules* **2004**, *37*, 590−596.
(33) Eckart, C. *Phys. Rev.* **1930**, *35*, 1303.
(34) For more details on this procedure, see for example: Coote, M. L.; Collins, M. A.; Radom, L. *Mol. Phys.* **2003**, *101*, 1329−1338.
(35) Coote, M. L. In *Encyclopedia of Polymer Science and Technology,* 3rd ed.; Kroschwitz, J. I., Ed.; John Wiley & Sons: New York, 2004; Vol. 9, pp 319−371.
(36) LLauro-Darricades, M.-F.; Guyot, A. *J. Macromol. Sci., Chem.* **1986**, *A23*, 221−269.
(37) Starnes, W. H., Jr.; Villacorta, G. M.; Schilling, F. C. *Polym. Prepr. (Am. Chem. Soc., Div. Polym. Chem.)* **1981**, *22*, 307−308.
(38) Wescott, L. D. *Macromolecules* **1984**, *17*, 2501−2507.
(39) Braun, D.; Sonderhof, D. *Eur. Polym. J.* **1982**, *18*, 141−148.
(40) (a) Bauer, J.; Sabel, A. *Angew. Makromol. Chem.* **1975**, *47*, 15−27. (b) George, M. H.; Garton, A. *J. Macromol. Sci., Chem. Ed.* **1977**, *A11*, 1389−1410. (c) Lederer, M. *Angew. Chem.* **1959**, *71*, 162.
(41) Pauwels, K. F. D.; Purmova, J.; Schouten, A. J. To be published.
(42) Starnes, W. H., Jr.; Wojciechowski, B. J. *Makromol. Chem., Macromol. Symp.* **1993**, *70/71*, 1−11.
(43) Rigo, A.; Palma, G.; Talamini, G. *Makromol. Chem.* **1972**, *153*, 219−228.
(44) Purmova, J.; Pauwels, K. F. D. Vorenkamp, J. E.; Schouten, A. J. To be published.
(45) Park, G. S.; Saleem, M. *Polym. Bull.* **1979**, *1*, 409−413.
(46) Starnes, W. H., Jr.; Schilling, F. C.; Abbås, K. B.; Cais, R. E.; Bovey, F. A. *Macromolecules* **1979**, *12*, 556−562.
(47) Nesmeyanov, A. N.; Freidlina, R. Kh.; Kost, V. N.; Khorlina, M. Ya. *Tetrahedron* **1961**, *16*, 94−125.
(48) Xie, T. Y.; Hamielec, A. E.; Wood, P. E.; Woods, D. R. *J. Appl. Polym. Sci.* **1987**, *34*, 1749−1766.
(49) Burnett, G. M.; Wright, W. W. *Proc. R. Soc. London* **1954**, *A221*, 41−53. Note also that values of $5.4 \pm 1.5 \times 10^3$ L mol^{-1} s^{-1} and 3.13×10^3 L mol^{-1} s^{-1} were reported at 25 °C by Kajiwara et al. *Macromol. Chem. Phys*. **2000**, *201*, 2165−2169 (using ESR) and Bengough et al. *Trans. Faraday Soc.* **1965**, *61*, 1735 (using rotating sector), respectively. In the paper of Burnett et al., the rotating sector method was used as well, and the value of 6.38×10^3 L mol^{-1} s^{-1} at 25 °C was reported. Using the same level of theory as the present work, we calculate a corresponding value of 2.8×10^3 L mol^{-1} s^{-1} at 25 °C, which is in excellent agreement with these literature values.
(50) Coote, M. L. *Aust. J. Chem.* **2004**, *57*, 1125−1132.
(51) Talamini, G.; Visentini, A.; Kerr, J. *Polymer* **1998**, *39*, 1879−1891.
(52) Ravey, M.; Waterman, J. A.; Shorr, L. M.; Kramer, M. *J. Polym. Sci., Polym. Chem. Ed.* **1974**, *12*, 2821−2843.
(53) See for example: (a) Hamielec, A. E. In *Science and Technology of Polymer Colloids*; Poehlein, G. W., Ottweil, R. H., Goodwin, J. W. E., Eds.; Martinus Nijhof Publishers: The Hague, **1983**; p 140. (b) Xie, T. Y.; Hamielec, A. E.; Wood, P. E.; Woods, D. R. *Polymer* **1991**, *32*, 537−557. (c) Kiparissides, C.; Daskalakis, G.; Achilias, D. S.; Sidiropoulou, E. *Ind. Eng. Chem. Res.* **1997**, *36*, 1253−1267.
(54) Smoluchowski, M. Z. *Phys. Chem.* **1918**, *92*, 129.
(55) Clay, P. A.; Gilbert, R. G. *Macromolecules* **1995**, *28*, 552−569.
(56) See for example: (a) Dullien, A. L. *AIChE J.* **1972**, *18*, 62−70. (b) Zielinski, J. M. *M*acromolecules **1996**, *29*, 6044−6047.
(57) Masaro, L.; Zhu, X. X. *Prog. Polym. Sci.* **1999**, *24*, 731−775.
(58) Bueche, F. *Physical Properties of Polymers*; Wiley-Interscience: New York, 1962.
(59) De Roo, T.; Heynderickx, G. J.; Marin, G. B. *Macromol. Symp.* **2004**, *206*, 215−228.
(60) Starnes, W. H., Jr.; Wojciechowski, B. J.; Chung, H.; Benedikt, G. M.; Park, G. S.; Saremi, A. H. *Macromolecules* **1995**, *28*, 945−949.
(61) Rigo, A.; Palma, G.; Talamini, G. *Makromol. Chem.* **1972**, *153*, 219−228.
(62) Starnes, W. H., Jr.; Wojciechowski, B. J.; Velazquez, A.; Benedikt, G. M. *Macromolecules* **1992**, *25*, 3638−3641.
(63) Starnes, W. H., Jr.; Chung, H.; Pike, R. D.; Wojciechowski, B. J.; Zaikov, V. G.; Benedikt, G. M.; Goodall, B. L.; Rhodes, L. F. *Polym. Prepr.* **1995**, *36*, 404−405.
(64) Lenz, R. W.; Feay, D. C.; Schneider, N. S. *Organic Chemistry of Synthetic High Polymers*; Wiley-Interscience: London, **1967**; pp 292−295.

MA050035P